PHYSICAL REVIEW A VOLUME 42, NUMBER 8 15 OCTOBER 1990

Continuous quantum measurements and chaos

T. Dittrich*
Department of Nuclear Physics, Weizmann Institute, Rehovot, Israel

R. Graham
Fachbereich Physik, Universität Gesamthochschule, Essen, Essen, West Germany
(Received 11 January 1990)

The quantized standard map (kicked rotor) is coupled to macroscopic systems acting as measuring devices for the probability distribution of the action variable or some of its moments. As a result of such measurements, which are continuous in time but have a limited time resolution, localization of the action variable is destroyed in sufficiently long time scales and replaced by diffusion. The diffusion constant, in general, differs from that of the classical chaotic diffusion and depends on the measurement performed.

I. INTRODUCTION

The quantum theory of measurements, founded by the work of von Neumann,[1] has seen a considerable revival of interest in recent years. An excellent source for the history of the subject is Ref. 2. In particular, the problem of measurements which are repeated in time or which are carried out continuously, has been discussed in a number of recent papers.[3–8] Among the motivations of such studies is the problem of the detection of gravitational waves, where it is necessary to monitor an interferometer continuously in time with a sensitivity reaching the quantum limit.[9] Further motivation stems from the recent interest in the quantum behavior of dynamical systems which are chaotic in their classical limit ("quantum chaos"). Practically, the standard way to detect chaos in a dynamical system is through a suitable analysis of a time series of data obtained by repeated measurements of a single dynamical variable. In quantum mechanics, however, the concept of a time series is more involved, since here the back reaction of each measurement on the dynamics has to be taken into account. The time evolution of a dynamical variable obtained, e.g., by numerical iteration of a quantum map describing the isolated system, neglects this altogether. In order to realize it experimentally, an ensemble would have to be discarded and prepared anew in the initial state after each measurement. An adequate quantum-mechanical analog of a classical time series consists in a periodic or continuous measurement performed on a single ensemble. However, a continuous observation profoundly changes the quantum dynamics. It has been stressed, particularly by Lamb,[10] that the clarification of "quantum chaos" requires the prior understanding of the concept of measurements in quantum mechanics.

In the present paper we wish to analyze in detail the theory of measurements that are continuous in time and, in particular, their effect on the dynamics of the observed system. This theory allows us to study how the quantum dynamics of a prototypical system that is chaotic in its classical limit, the kicked rotor (standard map), is modified by continuous observation. Basic ideas of our work are similar to those expounded on in Refs. 4–6, where applications to *linear* systems are given. Strong similarities of some of our goals also exist with those of Sarkar and Satchell,[7] who investigate the influence of destructive and continuous measurements on the time evolution of the quantized kicked rotor, coupled to a two-level system, on which, in turn, the measurements are performed. In contrast to Ref. 7, we study the effect of a *direct* coupling of the kicked rotor to a macroscopic measuring device. A feature of special interest in our present context is the dynamical localization[11] exhibited by the quantized standard map. As a typical quantum-mechanical interference effect, it is very sensitive to any incoherent perturbation, such as random noise[12] or the coupling to a macroscopic environment.[13–15] Repeated measurements, in particular, are effected by such couplings and are expected to disrupt localization.[14] While this effect could not be observed in the model studied in Ref. 7, we find that measurements performed directly on the kicked rotor do destroy localization on a sufficiently long time scale.

In Sec. II we consider the coupling of the measured dynamical system to a macroscopic measuring device and derive the corresponding nonunitary measured quantum dynamics. The response of the measuring device is analyzed in Sec. III. The application to the quantized standard map and our numerical results on its measured dynamics follow in Sec. IV, and in Sec. V we summarize our conclusions.

II. QUANTUM DYNAMICS OF A CONTINUOUSLY MEASURED SYSTEM

Let us consider a quantum system S described by the Hamiltonian H_S on which a measurement is to be performed continuously in time. Generally speaking, a measuring apparatus (meter) M is a macroscopic system[1] coupled to the system S in such a way that the classical measurement of a suitable macroscopic variable of M yields the desired information on S. To be specific, let

the coupling between the system and the meter be[1]

$$H_I=\hbar g X x\,\theta(t)\ , \tag{2.1}$$

where g is a coupling constant and X,x are some Hermitian linear operators acting in the Hilbert spaces of the meter and the system, respectively. The measurement starts at $t=0$, as indicated by the step function $\theta(t)$. Furthermore, let H_M be the Hamiltonian of the meter. It is conventional in measurement theory, to use instead of (2.1) a time-dependent Hamiltonian with δ functions. We believe that (2.1) is more realistic for measurements continuous in time.

We assume that X is defined in such a way that its expectation value vanishes for the uncoupled meter, and that the uncoupled meter is in some stationary state where multitime correlation functions depend on time differences only. Thus we define for the uncoupled meter in its Heisenberg picture $X=X^{(0)}(t)$,

$$\begin{aligned}&\langle X^{(0)}(t)\rangle=0\ ,\\ &\tfrac{1}{2}\langle X^{(0)}(t)X^{(0)}(t')+X^{(0)}(t')X^{(0)}(t)\rangle=S_x(t-t')\ ,\\ &\frac{1}{2\hbar}\langle X^{(0)}(t)X^{(0)}(t')-X^{(0)}(t')X^{(0)}(t)\rangle=\chi_x''(t-t')\ .\end{aligned} \tag{2.2}$$

From here on we restrict our attention to a special class of meters: We shall assume that the fluctuations of X in the meter have a correlation time

$$\tau_x=\frac{1}{\langle (X^{(0)})^2\rangle}\int_0^\infty d\tau S_x(\tau)\ , \tag{2.3}$$

which is much smaller that the characteristic time scales of the dynamics of S. In this case we may replace $S_x(t)$ by

$$S_x(t)=2\tau_x\langle (X^{(0)})^2\rangle\delta(t)\ . \tag{2.4}$$

Similarly, we assume that $\chi_x''(t-t')$ has a correlation time much smaller than the characteristic time scales of S. We may then replace

$$\chi_x''(\omega)=\int_{-\infty}^{\infty} dt\, e^{i\omega t}\chi_x''(t) \tag{2.5}$$

by

$$\chi_x''(\omega)\simeq\omega\gamma \tag{2.6}$$

in the frequency range of relevance for S, where γ is a positive constant. Taken together, these approximations amount to taking

$$\langle X^{(0)}(t)X^{(0)}(t')\rangle\simeq 2\tau_x\langle (X^{(0)})^2\rangle\delta(t-t')+i\hbar\gamma\frac{d}{dt}\delta(t-t')\ . \tag{2.7}$$

If the meter is a system in thermal equilibrium, the functions $S_x(t),\chi_x''(t)$ are related by the fluctuation dissipation theorem,

$$S_x(t)=\hbar\int d\omega\frac{1}{2\pi}e^{-i\omega t}\chi_x''(\omega)\coth\frac{\beta\hbar\omega}{2}\ . \tag{2.8}$$

The coefficients in Eq. (2.7) may then be expressed by

$$\begin{aligned}&\langle (X^{(0)})^2\rangle=\hbar\int d\omega\frac{1}{2\pi}\chi_x''(\omega)\coth\frac{\beta\hbar\omega}{2}\ ,\\ &\tau_x\langle (X^{(0)})^2\rangle=\hbar\int d\omega\frac{1}{2\pi i}\frac{\chi_x''(\omega)}{\omega}\coth\frac{\beta\hbar\omega}{2}\ ,\\ &\gamma=\lim_{\omega\to 0}\frac{\chi_x''(\omega)}{\omega}\ .\end{aligned} \tag{2.9}$$

A fundamental principle of quantum mechanics asserts that any measurement changes the state of the measured system in an irreversible way. This irreversibility is a consequence of the macroscopic nature of the meter M. As a consequence of this fundamental principle, measurements which are performed on S continuously in time change the state of S continuously in time, i.e., they turn the unmeasured dynamics into measured dynamics. We now formulate the measured dynamics under the assumptions made. As the state of S changes irreversibly it is not pure but a statistical mixture described by a statistical operator ρ. The unmeasured dynamics is given by von Neumann's equation

$$i\hbar\dot\rho=[H_S,\rho]\ . \tag{2.10}$$

The influence of the measuring device, for sufficiently weak coupling, can be described perturbatively in g in lowest (second) order. Using the interaction representation with respect to H_S+H_M we obtain in second-order perturbation theory

$$\begin{aligned}\tilde\rho_S(t)-\tilde\rho_S(0)=-g^2\int_0^t d\tau\int_0^\tau d\tau'[&\langle X^{(0)}(\tau)X^{(0)}(\tau')\rangle\tilde x(\tau)\tilde x(\tau')\tilde\rho_S(\tau')+\langle X^{(0)}(\tau')X^{(0)}(\tau)\rangle\tilde\rho_S(\tau')\tilde x(\tau')\tilde x(\tau)\\ &-\langle X^{(0)}(\tau)X^{(0)}(\tau')\rangle\tilde x(\tau')\tilde\rho_S(\tau')\tilde x(\tau)-\langle X^{(0)}(\tau')X^{(0)}(\tau)\rangle\tilde x(\tau)\tilde\rho_S(\tau')\tilde x(\tau')]\ .\end{aligned} \tag{2.11}$$

Here, $\tilde\rho_S$ and $\tilde x$ are ρ and x in the interaction representation. In Eq. (2.11) we took the trace over the Hilbert space of the meter assuming that the total statistical operator $\rho_{\rm tot}$ at time $t=0$ factorizes

$$\rho_{\rm tot}(0)=\rho(0)\otimes\rho_M(0)\ . \tag{2.12}$$

We also used the fact that $\langle X^{(0)}\rangle=0$. Within second order of g factorization of $\rho_{\rm tot}(\tau')$ may be used in Eq. (2.11) also at later times $\tau>0$. Making use now of Eq. (2.7) and differentiating once with respect to time we obtain

$$\dot{\tilde\rho}_S=g^2\tau_x\langle (X^{(0)})^2\rangle[\tilde x,[\tilde\rho_S,\tilde x]]+\tfrac{1}{2}g^2\gamma([\tilde x\tilde\rho_S,[H_S,\tilde x]]-[[H_S,\tilde x],\tilde\rho_S\tilde x])\ . \tag{2.13}$$

We can now transform back to the Schrödinger picture of the system $\hat S$ and obtain

$$\dot{\rho}=-\frac{i}{\hbar}[H_S,\rho]+g^2\tau_x\langle(X^{(0)})^2\rangle[x,[\rho,x]] +\tfrac{1}{2}g^2\gamma([x\rho,[H_S,x]]-[[H_S,x],\rho x]) , \tag{2.14}$$

describing the irreversible measured dynamics. Irreversibility arises from the second and third term on the right-hand side of Eq. (2.14). The second term represents incoherent fluctuations induced by the macroscopic meter on the system S. They lead to a diffusive spreading of the probability distribution in phase space. This interpretation can be substantiated by an estimate of the diffusion constant in terms of the parameters of the model: The diffusion constant is defined as

$$D=\frac{(\Delta p)^2}{\Delta t} , \tag{2.15}$$

where $(\Delta p)^2$ is the variance of the momentum canonically conjugate to the measured coordinate x. Accordingly, the uncertainty relation $\Delta p\Delta x\approx\hbar$ holds for this pair of variables and yields the estimate $(\Delta p)^2\approx\hbar^2/(\Delta x)^2$. Furthermore, we use the energy-time uncertainty relation $\Delta E\Delta t\approx\hbar$ to estimate $(\Delta x)^2$ in terms of system parameters: The energy scale relevant in this context is the energy exchange due to the interaction Hamiltonian (2.1), i.e., $\Delta E\approx\hbar gX\Delta x$, thus $(\Delta x)^2\approx 1/g^2\langle X^2\rangle(\Delta t)^2$. The time scale Δt is given by the correlation time τ_x of the meter so that, finally, we have

$$D\approx\hbar^2g^2\langle X^2\rangle\tau_x . \tag{2.16}$$

The third term in Eq. (2.14) describes a drift in the probability towards states with low energy, corresponding to dissipation. The effects of dissipation on classically chaotic quantum systems have been discussed in detail in Refs. 13–15. Therefore, in our applications in Sec. IV we shall use Eq. (2.14) only in the special case $\gamma=0$. This condition is satisfied if

$$\chi_x''(\omega)/\omega\approx 0 \tag{2.17}$$

holds in the frequency domain of relevance to the system S [cf. Eq. (2.6)].

III. RESPONSE OF THE MEASURING DEVICE

The macroscopic apparatus M can be used as a meter only if the interaction with S leads to a permanent modification of the state of M, which can be read off classically, i.e., without further perturbation of the system S. Let Y be the observable of M which is recorded. Its free dynamics (for the uncoupled meter) in the Heisenberg picture is

$$Y^{(0)}(t)\equiv U_0^\dagger(t)YU_0(t) , \tag{3.1}$$

with

$$Y^{(0)}(0)=Y , \quad U_0(t)=e^{-(i/\hbar)(H_S+H_M)t} \tag{3.2}$$

(with obvious modifications in the notation if H_S depends on time explicitly). Let us assume that Y is defined in such a way that $\langle Y^{(0)}(t)\rangle=0$. We are interested in the change

$$\delta Y(t)=Y(t)-Y^{(0)}(t) \tag{3.3}$$

due to the coupling to the system S. Here, $Y(t)$ is defined by the full dynamics in the Heisenberg picture

$$Y(t)=U^\dagger(t)YU(t) , \tag{3.4}$$

where

$$U(t)=e^{-(i/\hbar)(H_S+H_M+H_I)t} . \tag{3.5}$$

Then we have

$$Y(t)=\tilde{U}^\dagger(t)Y^{(0)}(t)\tilde{U}(t) \tag{3.6}$$

with

$$\tilde{U}(t)=U_0^\dagger(t)U(t) . \tag{3.7}$$

Hence

$$\dot{\tilde{U}}(t)=-\frac{i}{\hbar}U_0^\dagger(t)H_IU(t) =-igX^{(0)}(t)\tilde{U}(t)x(t) , \tag{3.8}$$

where $X^{(0)}(t)$ is the free dynamics defined in Eq. (3.1) and

$$x(t)=U^\dagger(t)xU(t) . \tag{3.9}$$

The integral equation

$$\tilde{U}(t)=1-ig\int_0^t d\tau X^{(0)}(\tau)x(\tau) \tag{3.10}$$

equivalent to Eq. (3.8) can be solved by its von Neumann series

$$\tilde{U}(t)=1+\sum_{n=1}^{\infty}(-ig)^n\int_0^t d\tau_n\int_0^{\tau_n}d\tau_{n-1}\cdots\int_0^{\tau_2}d\tau_1X^{(0)}(\tau_n)\cdots X^{(0)}(\tau_1)x(\tau_1)\cdots x(\tau_n) . \tag{3.11}$$

For simplicity we shall assume that the linear response gives a sufficiently accurate description, i.e., we neglect the terms with $n\geq 2$ in Eq. (3.11). Then we obtain for $\delta Y(t)$

$$\delta Y(t)=ig\int_0^t d\tau[x(\tau)X^{(0)}(\tau)Y^{(0)}(t) -Y^{(0)}(t)X^{(0)}(\tau)x(\tau)] . \tag{3.12}$$

As the right-hand side of (3.12) is already of first order in g we may neglect, to this order, the noncommutativity of $x(\tau)$ with $X^{(0)}(\tau), Y^{(0)}(t)$, caused by the coupling of M and S. Thus, within first order in g, Eq. (3.12) may be replaced by

$$\delta Y(t)=-ig\int_0^t d\tau[Y^{(0)}(t),X^{(0)}(\tau)]x(\tau) . \tag{3.13}$$

The measurement of Y yields a probability distribution of the measured values, which may be assumed Gaussian for a macroscopic system and can therefore be specified by its mean value $\langle Y(t)\rangle=\langle Y^{(0)}(t)\rangle+\langle\delta Y(t)\rangle$ and its variance $\Delta_Y=\langle(Y^{(0)})^2\rangle-\langle Y^{(0)}\rangle^2+\langle[\delta Y(t)]^2\rangle-\langle\delta Y(t)\rangle^2$, assuming that the fluctuations of $Y^{(0)}$ and δY are independent. For the mean value of δY we obtain from Eq. (3.13)

$$\delta\langle Y(t)\rangle=-ig\int_0^t d\tau\,\mathrm{Tr}\rho(0)\otimes\rho_M(0)\times[Y^{(0)}(t),X^{(0)}(\tau)]x(\tau)\ . \tag{3.14}$$

Here, $\rho_S(0),\rho_M(0)$ are the statistical operators of the system S and the meter M, respectively, at time $t=0$, when S is first brought into contact with M. The total statistical operator $\rho_{\mathrm{tot}}(t)$ factorizes at this time according to Eq. (2.12). By cyclic rearrangement under the trace we may rewrite Eq. (3.14) as

$$\delta\langle Y(t)\rangle=-ig\,\mathrm{Tr}\left[x\int_0^t d\tau\,\rho_{\mathrm{tot}}(\tau)U(\tau)\times[Y^{(0)}(t),X^{(0)}(\tau)]U^\dagger(\tau)\right]\ . \tag{3.15}$$

Again various simplifications are permitted if accuracy is only required to first order in g: We may replace $U(\tau)$ by $U_0(\tau)$ as both operators differ only to first and higher order in g, and we may factorize $\rho_{\mathrm{tot}}(\tau)\simeq\rho(\tau)\otimes\rho_M(\tau)$ to the same order. Then the trace in Eq. (3.15) can be factorized into separate traces over the system and the reservoir, and we obtain finally

$$\langle Y(t)\rangle=\delta\langle Y(t)\rangle\simeq-\hbar g\int_0^t d\tau\,\chi_{YX}(t-\tau)\langle x(\tau)\rangle \tag{3.16}$$

with the linear-response function

$$\chi_{YX}(t)=\frac{i}{\hbar}\mathrm{Tr}\rho_M[Y^{(0)}(t),X^{(0)}]\theta(t)\ , \tag{3.17}$$

where $\theta(t)$ is the step function and where we made use of $\langle Y^{(0)}(t)\rangle=0$. The variance may be obtained similarly starting from Eq. (3.13), with the result

$$\langle[\delta Y(t)]^2\rangle=\hbar^2g^2\int_0^t d\tau' K(t-\tau,t-\tau')\langle x(\tau)x(\tau')\rangle\ , \tag{3.18}$$

where

$$K(t-\tau,t-\tau')=\left[\frac{i}{\hbar}\right]^2\langle[Y^{(0)}(t),X^{(0)}(\tau)][Y^{(0)}(t),X^{(0)}(\tau')]\rangle\theta(t-\tau)\theta(t-\tau')\ . \tag{3.19}$$

Assuming Gaussian statistics for the free meter, we obtain from (3.19) by Gaussian factorization

$$K(t-\tau,t-\tau')=\chi_{YX}(t-\tau)\chi_{YX}(t-\tau')\ . \tag{3.20}$$

Hence

$$\Delta_Y=\Delta_Y^{(0)}+\hbar^2g^2\int_0^t d\tau\int_0^t d\tau'\chi_{YX}(t-\tau)\chi_{YX}(t-\tau')\langle[x(\tau)-\langle x(\tau)\rangle][x(\tau')-\langle x(\tau')\rangle]\rangle\ , \tag{3.21}$$

where $\Delta_Y^{(0)}$ is the variance of Y for the free meter. A good measurement requires $\Delta_Y^{(0)}$ to be smaller than $\langle Y(t)\rangle^2$ if the expectation $\langle x(t)\rangle$ is measured, and smaller than $(\Delta_Y-\Delta_Y^{(0)})$ if the probability distribution of $x(t)$ is to be resolved. At the same time the response function $\hbar g\chi_{YX}$ should be as large as possible. The general uncertainty relation (for systems which are stationary)

$$\langle(X^{(0)})^2\rangle\Delta_Y^{(0)}\geq\tfrac{1}{4}|\langle[Y(t),X(\tau)]\rangle|^2=\frac{\hbar^2}{4}|\chi_{YX}(t-\tau)|^2 \tag{3.22}$$

follows from the Schwarz inequality. It places a fundamental limit on time-resolved measurements. It states that a good measurement ($\hbar^2g^2|\chi_{YX}|^2$ large, $\Delta_Y^{(0)}$ small) necessarily implies that $g^2\langle(X^{(0)})^2\rangle$ must be sufficiently large. However, it is precisely this latter parameter, together with the (short) correlation time τ_x, which governs the magnitude of the irreversible part of the measured dynamics [cf. Eq. (2.14)]. The precision of the measurement and the back action on the system are therefore inextricably connected in the way typical for quantum mechanics.

IV. MEASUREMENTS OF THE ACTION VARIABLE OF THE QUANTIZED STANDARD MAP

A. Master equation of the measured dynamics

The standard map is the paradigm of a classical Hamiltonian system capable of chaotic behavior.[16] Its dynamics is generated by the Hamiltonian

$$H_S(p,q;t)=\frac{p^2}{2}-\frac{K}{(2\pi)^2}\cos(2\pi q)\sum_{n=-\infty}^{\infty}\delta(t-n) \tag{4.1}$$

with the action variable p, the angle variable q, and the nonlinearity parameter K. Global chaos is observed for $K\gtrsim1$. It manifests itself by a diffusion of p. Equation (4.1) may be interpreted as the Hamiltonian of a periodically kicked rotor. The units of time and action are chosen such that the kicking period and the moment of inertia of the rotor are unity, respectively. The system (4.1) is easily quantized[11] by the canonical rule

$$[p,q]=-i\hbar\ . \tag{4.2}$$

For the system (4.1) it is most interesting to measure p or functions of p, because their time evolution indicates the presence or absence of dynamical localization.[11] We shall consider therefore interaction Hamiltonians (2.1) of the form

$$H_I^{(1)}=\hbar g X f(p/2\pi\hbar)\theta(t) \tag{4.3}$$

or

$$H_I^{(2)}=\hbar\sum_l g_l X_l |l\rangle\langle l|\theta(t)\ , \tag{4.4}$$

where $f(l)=f(p/2\pi\hbar)$ is some function of p, measured in quanta $2\pi\hbar$, e.g., $f(l)=l$ or $f(l)=l^2$, and the states $|l\rangle$ are the eigenstates of p:

$$p|l\rangle=2\pi\hbar l|l\rangle,\ l \text{ integer}\ , \tag{4.5}$$

which are given, in q representation, by

$$\langle q|l\rangle=e^{i2\pi lq}\ . \tag{4.6}$$

g_l and X_l are as g and X in Eq. (2.1). In contrast to the models we discussed until now, $H_I^{(2)}$ describes the coupling of several meter variables X_l to the system. In order to resolve the individual expectation values $\langle l|\rho|l\rangle$ of $|l\rangle\langle l|$, it is then necessary to measure also several meter variables Y_l. The linear-response theory of Sec. III may easily be extended to this case. Equation (4.3) describes a measurement of $\langle f(p/2\pi\hbar)\rangle$, and Eq. (4.4) leads to a measurement of $\langle l|\rho|l\rangle=W_l$, the probability distribution of p. We shall assume that $\chi_x''(\omega)/\omega\simeq 0$ in the frequency domain of interest; i.e., dissipative effects are absent. From the Hamiltonian (4.3) we then obtain the master equation

$$\dot\rho=-\frac{i}{\hbar}[H_S,\rho]+\frac{g^2\tau_x}{2}\langle X^2\rangle_M[f(l),[\rho,f(l)]]\ , \tag{4.7}$$

while (4.4) with $\chi''_{x_l x_{l'}}(\omega)/\omega\simeq 0$ yields

$$\dot\rho=\frac{i}{\hbar}[H_S,\rho]+\sum_{l,l'}\frac{g_l g_{l'}}{2}\tau_{ll'}\langle X_l X_{l'}\rangle_M \times[|l\rangle\langle l|,[\rho,|l'\rangle\langle l'|]]\ . \tag{4.8}$$

Here and in the following, averages for the uncoupled meter are denoted by $\langle\cdots\rangle_M$. The relaxation times $\tau_{ll'}$ are defined in analogy to Eq. (2.3). They are assumed to be short compared to the time scale on which $W_l=\langle l|\rho|l\rangle$ evolves. It is convenient to rewrite Eqs. (4.7) and (4.8) in the l representation, where they take the form

$$\langle l|\dot\rho|m\rangle=-i2\pi^2\hbar(l^2-m^2)\langle l|\rho|m\rangle + \frac{iK}{4\pi^2\hbar}(\langle l+1|\rho|m\rangle+\langle l-1|\rho|m\rangle-\langle l|\rho|m+1\rangle-\langle l|\rho|m-1\rangle)\sum_{n=-\infty}^{\infty}\delta(t-n)+\left[\frac{\partial\langle l|\rho|m\rangle}{\partial t}\right]_{\rm inc}\ . \tag{4.9}$$

The last term in Eq. (4.9) represents the incoherent component in the measured dynamics, i.e.,

$$\left[\frac{\partial\langle l|\rho|m\rangle}{\partial t}\right]_{\rm inc}=-\frac{g^2\tau_x}{2}\langle X^2\rangle_M \times[f(l)-f(m)]^2\langle l|\rho|m\rangle \tag{4.10}$$

in the case of Eq. (4.7), and

$$\left[\frac{\partial\langle l|\rho|m\rangle}{\partial t}\right]_{\rm inc}=-\tfrac{1}{2}(g_l^2\tau_{ll}\langle X_l^2\rangle_M+g_m^2\tau_{mm}\langle X_m^2\rangle_M -2g_l g_m\tau_{lm}\langle X_l X_m\rangle_M)\langle l|\rho|m\rangle \tag{4.11}$$

for Eq. (4.8). For simplicity we shall only consider the case where

$$\langle X_l X_m\rangle_M=\langle X^2\rangle_M\delta_{lm},\quad \tau_{ll}=\tau_c,\quad g_l=g\ . \tag{4.12}$$

Equation (4.11) then reduces to

$$\left[\frac{\partial\langle l|\rho|m\rangle}{\partial t}\right]_{\rm inc}=-g^2\tau_c\langle X^2\rangle_M(1-\delta_{lm})\langle l|\rho|m\rangle\ . \tag{4.13}$$

It is easy to solve Eq. (4.9) with (4.10) and (4.13) over one period of the kicks. The master equation then reduces to a discrete map, which describes the measured dynamics of the quantized standard map. We obtain

$$\langle l|\rho_{n+1}|m\rangle=\sum_{l',m'}b_{l-l'}\left[\frac{K}{4\pi^2\hbar}\right]b^*_{m-m'}\left[\frac{K}{4\pi^2\hbar}\right]\times\langle l'|\tilde\rho_{n+1}|m'\rangle \tag{4.14}$$

with

$$\langle l|\tilde\rho_{n+1}|m\rangle=\exp\{-i2\pi^2\hbar(l^2-m^2)-\tfrac{1}{2}g^2\tau_x\langle X^2\rangle_M \times[f(l)-f(m)]^2\}\langle l|\rho_n|m\rangle \tag{4.15}$$

in the case where $\langle f(p)\rangle$ is measured, and

$$\langle l|\tilde\rho_{n+1}|m\rangle=\begin{cases}\exp[-i2\pi^2\hbar(l^2-m^2)-g^2\tau_c\langle X^2\rangle]\langle l|\rho_n|m\rangle & (l\neq m)\\ \langle l|\rho_n|m\rangle & (l=m)\end{cases} \tag{4.16}$$

if the probability distribution of p is measured. $b_l(x)$ in Eq. (4.14) are Bessel function defined by

$$b_l(x)=\int_0^1 dq\, e^{-i[2\pi q l - x\cos(2\pi q)]} . \tag{4.17}$$

Several remarks are in order. First of all, the form of the master equation describing the measured dynamics depends on what is measured. This can be seen from the difference between Eqs. (4.7) and (4.8) or more explicitly between Eqs. (4.10) and (4.13). As a second remark we point out that the dissipationless measurements both of $\langle f(l)\rangle$ and of the probability distribution of p, which we described here, have a direct influence only on the off-diagonal elements of the density matrix in l representation. This is shown by the form of Eqs. (4.10) and (4.13). The diagonal elements of ρ are affected only indirectly through their coupling to the off-diagonal elements via the kicks, as described by Eq. (4.9). In the absence of kicks, p is conserved even under the coupling between system and reservoir. If dissipation is admitted, it also has a direct influence on the diagonal elements $\langle l|\rho|l\rangle$. For a closely related case where dissipation in the quantized standard is treated, cf. Refs. 14–16. Thirdly, we emphasize that Eqs. (4.9)–(4.13) provide a time-resolved description of the process of destruction of coherence during a measurement which contains the traditional quantum-mechanical concept of a collapse of the wave function as a limiting case. For example, if a function $f(l)$ is measured, coherence is completely destroyed if the exponential decay in Eq. (4.15) is complete in a single time step for all off-diagonal elements, i.e., if $g^2\tau_x\langle X^2\rangle[f(l)-f(m)]^2\gg 1$. Similarly, in the case of Eq. (4.16) complete collapse of the wave function occurs for

$$g^2\tau_x\langle X^2\rangle_M \gg 1 . \tag{4.18}$$

This result is consistent with our estimate (2.16) for the rate of diffusion due to incoherent perturbations. To make this clear we note that the phase q is canonically conjugate to the measured variable $p=2\pi\hbar l$ in the present example. Therefore, Eq. (2.15) refers to phase diffusion in this case. Indeed the collapse of the wave function after the measurement of l corresponds to a complete loss of phase information, i.e., to a diffusive spreading of the phase q over the entire unit circle. As x in Eq. (2.1) refers to classical units, while $p/2\pi\hbar$ or $|l\rangle\langle l|$ in (4.3) or (4.4) refer to quantum units, an additional factor $\hbar^2$ appears in Eq. (2.16).

From the point of view of the present work the most interesting case is, of course, the one where a complete reduction of the density matrix does not occur in a single time step. However, even if a complete reduction occurs, it is still possible to control the disturbing effect of the measurement if measurements are not performed during each time step but instead periodically only after Γ time steps, with $\Gamma\geq 1$, integer. In such a model, localization would be disrupted for $\Gamma\lesssim n^*$, the localization time,[11] as has been briefly discussed in Ref. 17 and studied analytically and numerically in Ref. 14.

We finally mention that a stroboscopic description of the measured dynamics in the form of a quantum map as in Eqs. (4.14)–(4.16) may be interpreted independently of the specific continuous dynamics between subsequent snapshots, from which it was derived. In particular, the master equations (4.14)–(4.16) can be arrived at also from a different model where the coupling of the system to the meter depends on time as a periodic δ function, similar to the driving force of the rotator itself [cf. eq. (4.1)].

B. Semiclassical limit

Let us consider the asymptotic behavior of the quantum maps (4.14)–(4.16) for small $\hbar$ (semiclassical limit). It is then useful to introduce the Wigner function for a cylindrical phase space[15,18]

$$W_n(l,q)=\sum_{l_1,l_2}\frac{\sin[\pi(l_1+l_2-2l)]}{\pi(l_1+l_2-2l)}e^{2\pi i(l_1-l_2)q} \times\langle l_1|\rho_n|l_2\rangle . \tag{4.19}$$

The quantum map can then be written as

$$W_{n+1}(l',q')=\sum_l\int_0^1 dq\, G_W(l',q'|l,q)W_n(l,q) . \tag{4.20}$$

The kernel G_W is kind of Fourier transform of the kernel G, which in turn is defined by rewriting the maps (4.14)–(4.16) as

$$\langle l'|\rho_{n+1}|m'\rangle=\sum_{l,m}G(l',m'|l,m)\langle l|\rho_n|m\rangle . \tag{4.21}$$

Explicitly, we find

$$G_w(l',q'|l,q)=\sum_{l_1',l_2',l_1,l_2}G(l_1',l_2'|l_1,l_2)e^{2\pi i[(l_1'-l_2')q'-(l_1-l_2)q]}\frac{\sin[\pi(l_1'+l_2'-2l')]}{\pi(l_1'+l_2'-2l')}\frac{\sin[\pi(l_1+l_2-2l)]}{\pi(l_1+l_2-2l)} . \tag{4.22}$$

The kernel G_W can be simplified considerably in the limit where $\hbar\to 0, l\to\infty, l'\to\infty$, with $p=2\pi\hbar l, p'=2\pi\hbar l'$ held fixed. In this limit $\sum_l\to\int dp(1/2\pi\hbar)$. As shown in the Appendix, G_W then reduces to

$$G_W\left[\frac{p'}{2\pi\hbar},q'\middle|\frac{p}{2\pi\hbar},q\right]\simeq 2\pi\hbar\,\delta\left[p'-\left[p-\frac{K}{2\pi}\sin(2\pi q')\right]\right]\times g(q'-(q+p)) , \tag{4.23}$$

with

$$g(q)=\sum_{m=-\infty}^{\infty}\frac{1}{\sqrt{2\pi\Delta(p)}}\exp\left[-\frac{(q-m)^2}{2\Delta(p)}\right] , \tag{4.24}$$

$$\Delta(p)=(2\pi\hbar)^2g^2\tau_x\langle(X^{(0)})^2\rangle[f'(l)]^2$$

for the case where $\langle f(l)\rangle$ is measured, and

$$g(q)=1-\lambda+\lambda\sum_{m=-\infty}^{\infty}\delta(q-m)\ ,$$
$$\lambda=e^{-g^2\tau_c\langle X^2\rangle_M} \tag{4.25}$$

if $W(p)\sim\langle l|\rho|l\rangle$ is measured. It may be more transparent to rewrite the semiclassical limit of the maps in the form of a stochastic standard map,[19,20]

$$p_{n+1}=p_n-\frac{K}{2\pi}\sin(2\pi q_{n+1})\ ,$$
$$q_{n+1}=q_n+p_n+\xi_n\ , \tag{4.26}$$

with the Gaussian random variable ξ_n satisfying

$$\langle\xi_n\rangle=0\ ,$$
$$\langle\xi_n\xi_{n'}\rangle=\Delta(p)\delta_{nn'}\ , \tag{4.27}$$

in the case where $\langle f(l)\rangle$ is measured, and

$$\xi_n=0,\ \text{with probability } 1-\lambda$$
$$\xi_n\ \text{equidistributed in } [0,1),\ \text{with probability } \lambda \tag{4.28}$$

when $W(p)$ is measured.

C. Numerical results

We have solved numerically the master equations for the measured dynamics of the quantized standard map derived in Sec. IV A and their semiclassical limits derived in Sec. IV B and the Appendix. The results obtained for the case where the distribution function of the action is measured is fairly typical for the other cases, too, and therefore we shall consider mostly this case. Let us begin with the case of strong coupling between the system and the meter. A convenient measure for the coupling strength is the parameter

$$\nu=1-\lambda=1-\exp(-g^2\tau_x\langle(X^{(0)})^2\rangle)\ . \tag{4.29}$$

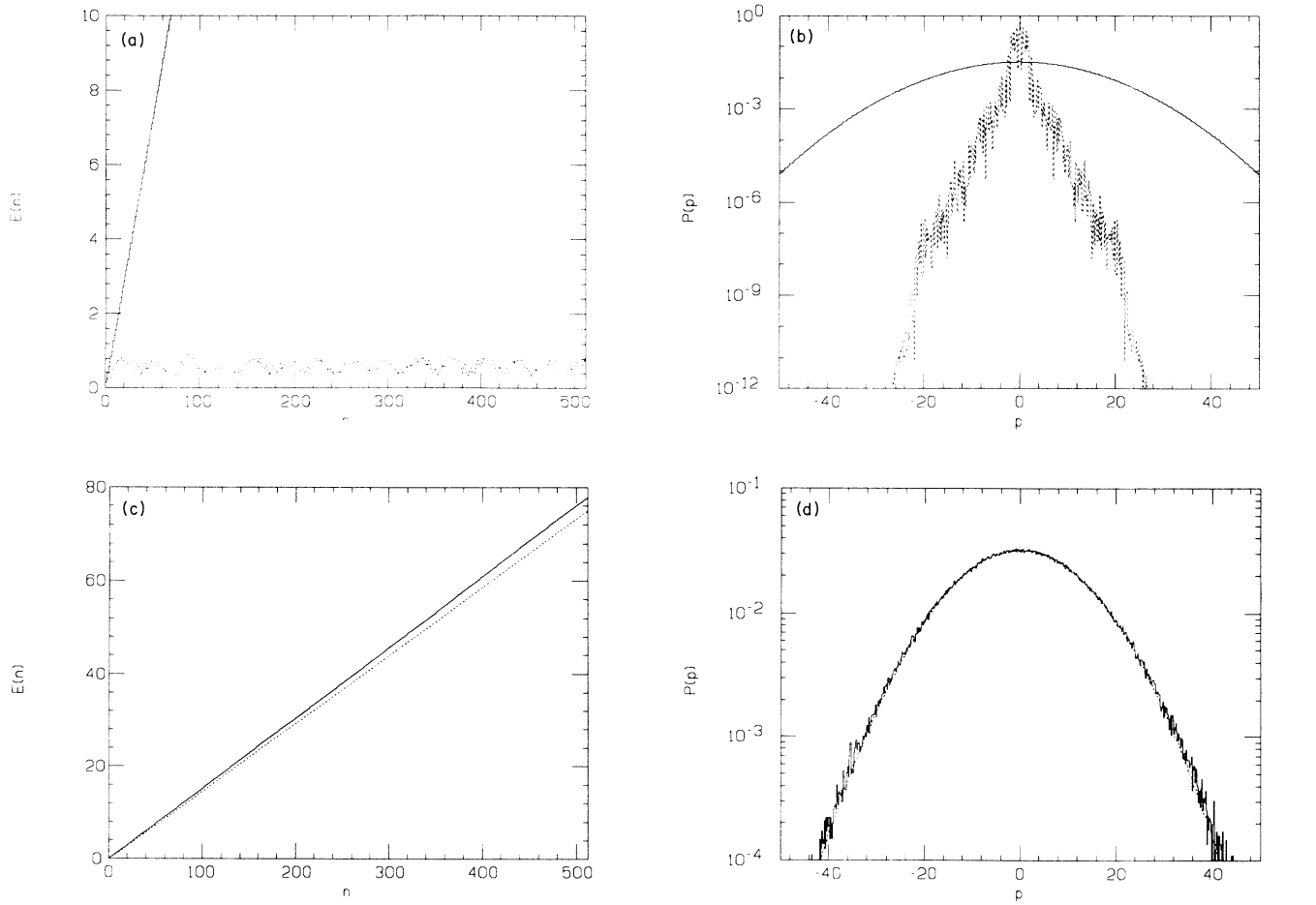

FIG. 1. Comparison of the measured dynamics of the quantized standard map with the corresponding unmodified dynamics of the same system [(a) and (b)] and with the stochastic map (4.25)–(4.27) [(c) and (d)]. The parameter values are $K=5$, $2\pi\hbar=0.1/[(\sqrt{5}-1)/2]$, and $\nu=0.5$ (for the measured dynamics). It is assumed that the complete probability distribution of the action variable p is measured. (a) shows the evolution of the mean energy for the measured (solid line) and unmeasured quantum dynamics (dotted line). (b) shows the action distribution after 512 time steps for the same two cases. The corresponding functions for the semiclassical approximation of the measured dynamics (solid line), compared with the exact result (dotted line), are shown in (c) and (d), respectively. Note that the dotted line in parts (c) and (d) represents the same data as the solid line in parts (c) and (d), respectively.

For $\nu=0$ the coupling vanishes, for $\nu=1$ the coupling dominates. In Fig. 1 we show results obtained for the case $K=5$ (regime of global chaos of the standard map) $2\pi\hbar=0.1/\gamma$, where $\gamma=(\sqrt{5}-1)/2$ (avoiding quantum resonance in the quantized standard map), and $\nu=0.5$ (case of strong coupling). In Fig. 1(a) the expectation value $E(n)=\langle p_n^2\rangle/2$ is plotted for the measured dynamics (solid line) and the unmeasured dynamics (dotted line). The initial state is the l eigenstate with $l=0$. The unmeasured dynamics exhibits the familiar time evolution generated by the quantized standard map, i.e., an initial diffusive growth of $E(n)$ followed by localization [saturation of $E(n)$]. The measured dynamics shows no trace of localization. Rather, as a result of the measurement, the initial diffusive growth of $E(n)$ continues unabated. In Fig. 1(b) the probability distribution of $l=p/2\pi\hbar$ obtained after 512 kicking periods is shown as a logarithmic plot, both for the measured case (solid line) and the unmeasured case (dotted line). Localization and its disruption are visible in the dotted and solid curves, respectively. In Figs. 1(c) and 1(d) we compare the semiclassical description of the measured dynamics (solid curve) and its full description by the master equation (dotted curve). We observe in Fig. 1(c) that the semiclassical description slightly overestimates the diffusion constant. As can be seen from Fig. 1(d), this overestimation is due to a slight systematic discrepancy in the wings of the probability distributions, which contribute rather strongly to the moment $\langle p^2\rangle$. In spite of this slight difference, the semiclassical description, in the present case, is simple and rather quantitative. The diffusion constant can be estimated very simply from Eqs. (4.27)–(4.29) by noting that both classical chaos and the additional fluctuations due to the measurement tend to randomize the phase variable and to destroy its correlations between different kicks. Hence, p diffuses, according to Ref. 21, as

$$\langle (p_{n+1}-p_n)^2\rangle=\frac{K^2}{(2\pi)^2}\langle \sin^2(2\pi q_n)\rangle\simeq\frac{1}{2}\frac{K^2}{(2\pi)^2}=D_{\rm ql}\ . \tag{4.30}$$

That is, the quasilinear approximation[21] of the classical diffusion constant is exactly valid here and holds even for $K<K_c$ (cf. the case $K=0.5$ discussed below). The Gaussian form of the probability distribution of p expected from this mechanism can be seen to be almost exactly realized in Fig. 1(d).

This simple argument also indicates that for sufficiently strong coupling, diffusion of p should result even if the classical map is not chaotic ($K<1$). This is checked in Fig. 2, where we choose the same parameters as in Fig. 1 except that now $K=0.5$, where the classical map is not

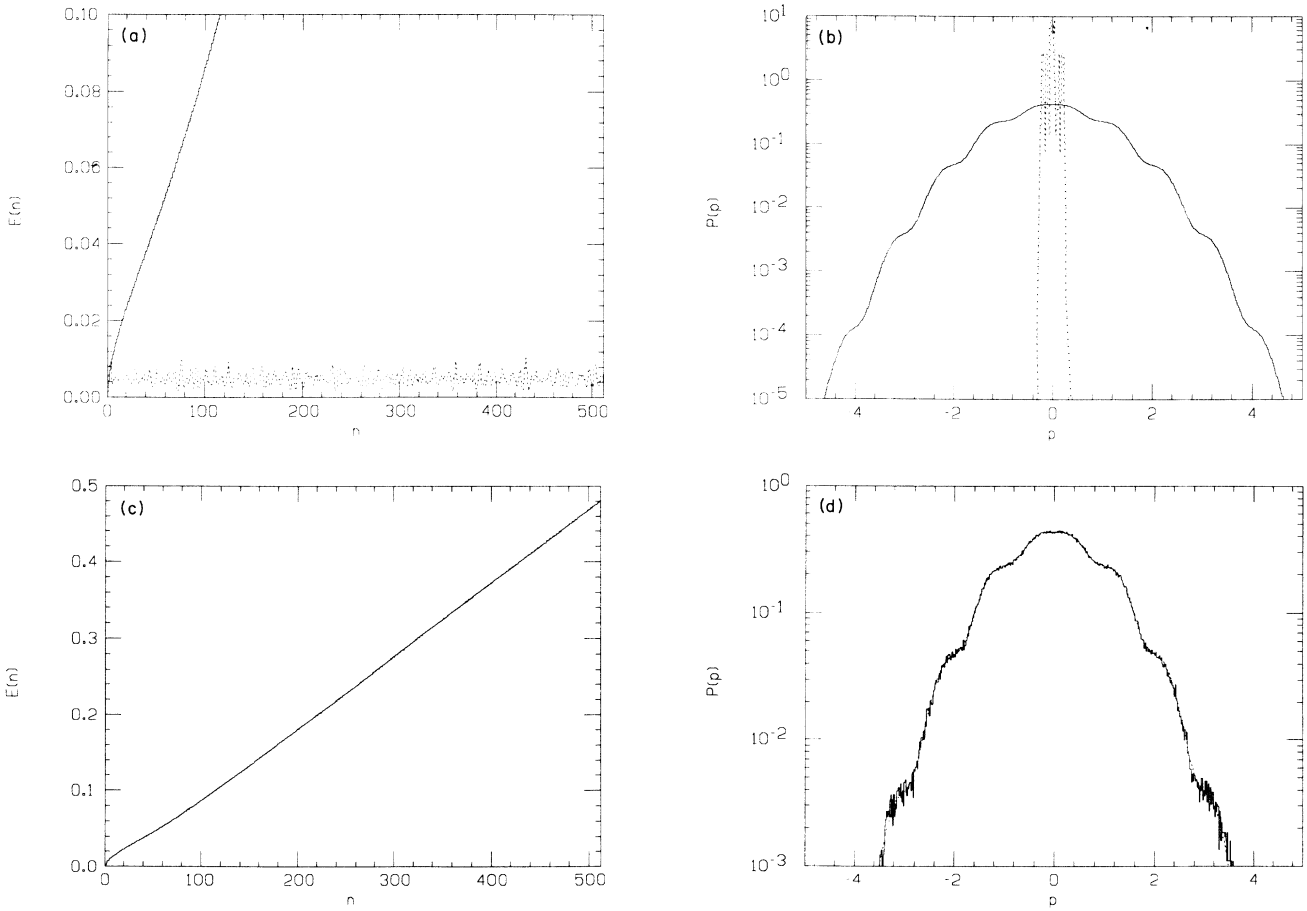

FIG. 2. Same as Fig. 1, but for $K=0.5$, where the classical standard map is mainly regular, and $2\pi\hbar=0.01/[(\sqrt{5}-1)/2]$.

globally chaotic, and $\hbar=0.01/\gamma$. Figures 2(a)–2(d) have the same format as Fig. 1. We see in Fig. 2(a) that the unmeasured quantum dynamics is localized, but the measured quantum dynamics is diffusive. The same difference can be seen in the distribution functions in Fig. 2(b). The diffusion of the measured dynamics is quantitatively described by the semiclassical limit as shown in Fig. 2(c), where no difference between the result of the master equation (solid curve) and the semiclassical result (dotted curve) can be seen. The same quantitative agreement can be seen in the distribution functions in Fig. 2(d). These distribution functions show, as an additional interesting feature, periodic steps superimposed on the global Gaussian decay. The coincidence of their period with the period $\Delta p=1$ of the classical standard map suggests that they occur as a consequence of the inhomogeneity of the classical phase space. Indeed, classically for $K<K_c$, jumping at random from one invariant torus to some neighbored one will be a more efficient transport mechanism near the fundamental resonances at $p=0,\pm1,\pm2\ldots$. The regions near $p=\pm\frac{1}{2},\pm\frac{3}{2},\ldots$, where phase space is less disturbed and invariant tori encircling the cylindrical phase space still dominate, act as partial barriers even for a noise-induced flow.

Now we turn to the case of weak coupling. In Figs. 3 and 4 we show results for the case $\nu=1-\lambda=10^{-4}$. In Fig. 3 we consider the case $K=5$ and also choose all other parameters, except ν, and the format as in Fig. 1. In Fig. 3(a) localization can be seen to be present in the measured dynamics (solid curve), which is very similar to the unmeasured dynamics (dotted curve). We emphasize, however, that the mean energy of the measured dynamics increases systematically compared to the unmeasured dynamics, and localization gives way to diffusion only for times n_c much longer than the $n=512$ kicking periods shown in the figure. The time n_c where localization gives way to diffusion and the quantum diffusion constant D_{qm} can be estimated from the master equation as in Refs. 14–16, and we find

$$n_c \simeq \frac{1}{1-\lambda}\ , \qquad D_{qm} \simeq D_{\mathrm{ql}}\frac{n^*}{n_c}\quad (\text{for } n_c > n^*)\ , \tag{4.31}$$

where

$$n^*=2L \tag{4.32}$$

is the number of kicking periods after which localization becomes manifest in the unmeasured dynamics, and

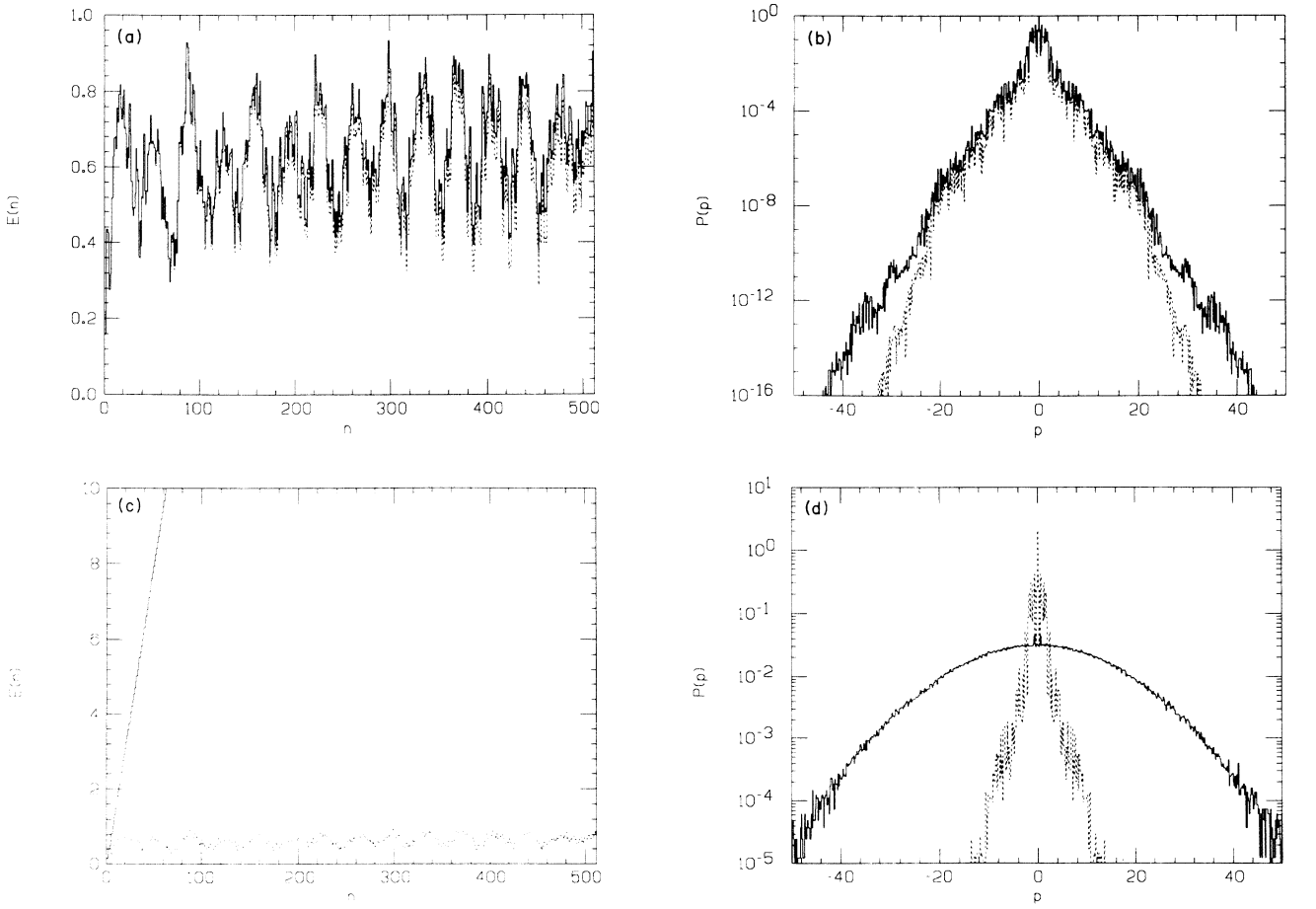

FIG. 3. Same as Fig. 1, but for weak coupling $\nu=10^{-4}$.

$$L \simeq \left[\frac{K}{4\pi^2 \hbar} \right]^2 \tag{4.33}$$

is the localization length. For the parameter values chosen in Fig. 3 we obtain $n_c \simeq 10^4$, $n^* \simeq 50$, $L \simeq 25$, $D_{qm} \simeq 0.25 \times 10^{-2} D_{ql}$. The systematic difference between the measured and the unmeasured dynamics can also be seen in the distribution functions in Fig. 3(b). The semiclassical approximation to the measured dynamics fails completely, as shown by Figs. 3(c) and 3(d). It misses entirely the localization effect. Indeed, the approximation of the integral over the classical action p by the δ function in Eq. (4.24) eliminates all effects of quantum coherence and hence of localization. Since ν is very small, chaos is the dominant mechanism of diffusion in the semiclassical description.

In the case of $K=0.5$, $\hbar=0.01/\gamma$, and $\nu=10^{-4}$ shown in Fig. 4, classical chaos is absent. Hence, in the full quantum-mechanical description of the measured dynamics [Figs. 4(a) and 4(b)], and even in its semiclassical approximation [Figs 4(c) and 4(d)], diffusion can only come about through the weak quantum noise associated with the coupling to the meter, and is not discernible during the time span shown. Accordingly, the semiclassical approximation captures correctly the time-averaged behavior, but it misses the strong quantum fluctuations around the averaged dynamics, which is now the dominating quantum coherence effect. The comparison of the measured with the unmeasured dynamics in Figs. 4(a) and 4(b) shows the same systematic discrepancies as in the case $K=5$ (Fig. 3).

In Fig. 5 we still consider a case of weak coupling, but this time we assume that only the energy is measured. Therefore, we now show solutions of the master equation (4.9) and (4.10).

The parameter λ of the coupling strength between system and meter is in this case given by

$$\lambda = \exp\left[\frac{g^2 \tau_x \langle (X^{(0)})^2 \rangle}{2(2\pi\hbar)^4} \right] . \tag{4.34}$$

In Fig. 5 we have chosen $\nu = 1-\lambda = 10^{-6}$ but we emphasize that the coupling mechanism is now quite different from that of Figs. 1–4 and the present value of λ therefore cannot be directly compared with the earlier values. Indeed the magnitude of the effective coupling matrix element now increases proportional to the mean action p and to the action difference, which explains why even very small values of $1-\lambda$ such as 10^{-6} now lead to

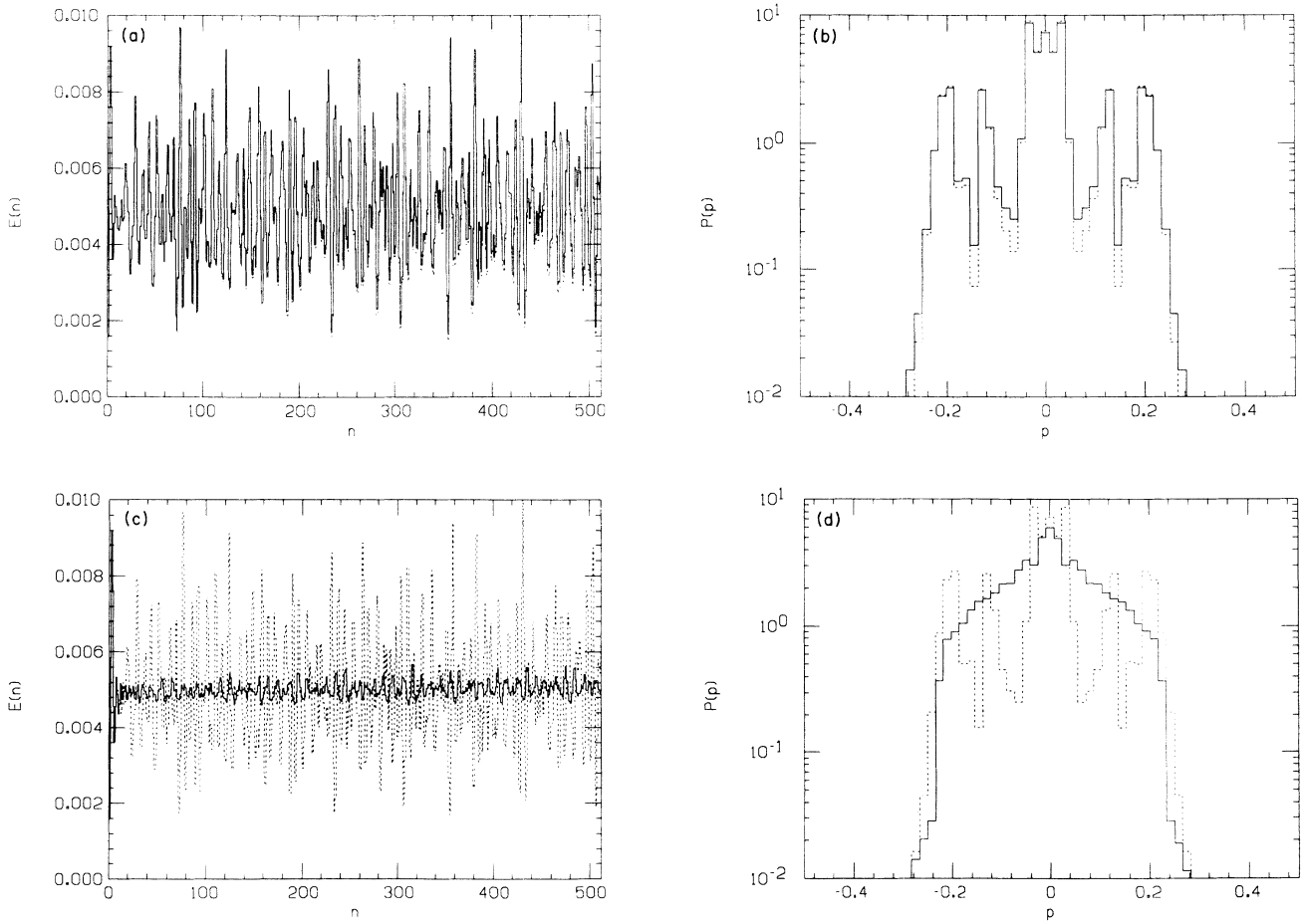

FIG. 4. Same as Fig. 2, but for weak coupling $\nu = 10^{-4}$.

stronger coupling on average as, e.g., $1-\lambda \simeq 10^{-4}$ in Fig. 3.

In Fig. 5(a) we see that also in this case the measured dynamics (solid line) deviates strongly from the unmeasured dynamics. The growth of the measured energy is seen to be superdiffusive. The reason is that, due to the p^2 coupling in H_I, the coupling strength between system and meter, and hence the transition rate between quasienergy levels, increases with increasing $\langle p^2 \rangle$. The superdiffusive increase of the measured E is still far slower than the diffusive chaotic increase which dominates the semiclassical description, as can be seen in Fig. 5(c).

In Figs. 5(b) and 5(d) we also show the distribution functions after 512 time steps, even though these would have to be measured (only once after 512 steps) by a second meter not included in our description. The absence of localization in the distribution of the measured dynamics in Fig. 5(b) and the overestimation of the diffusive spreading by the semiclassical approximation are already familiar from the results discussed before. New is a rather strong contribution to the probability distribution of the measured dynamics at and near to $p=0$. It appears that the measured system remains frozen at or near the initial state with rather high probability. The reason is again the coupling $\sim p^2$ between system and meter which turns off for $p \to 0$. Hence, quantum coherence and localization near $p=0$ are rather long-lived effects. Similar effects have been found earlier in the dissipative quantized standard map with p proportional friction.[13-15]

Finally, in Fig. 6 we study the effect of repeated measurements on quantum resonances[22,23] in the quantized standard map. They occur for rational values of the effective Planck's constant $2\pi\hbar$, introduced in Eq. (4.2) and are characterized by a continuous Floquet spectrum and extended Bloch-like eigenstates.

Figures 6(a) and 6(b) are analogous to Figs. 1(a) and 1(b) respectively, the only difference being that in the case shown here the parameter $2\pi\hbar$ is chosen as a simple rational, $2\pi\hbar=\frac{1}{4}$, and the coupling strength is $\nu=0.01$. In Fig. 6(a), the dotted line now shows the typical quadratic, i.e., superdiffusive increase of energy, in the unmeasured case. It replaces the saturation of energy growth characteristic of the nonresonant case [cf. Fig. 1(a)]. Quantum resonances are interference effects, like localization, and are likewise very sensitive to incoherent perturbation. Indeed, continuous measurements again lead, after a characteristic time, to a restoration of linear diffusion, visible in the solid line in Fig. 6(a). However, while for

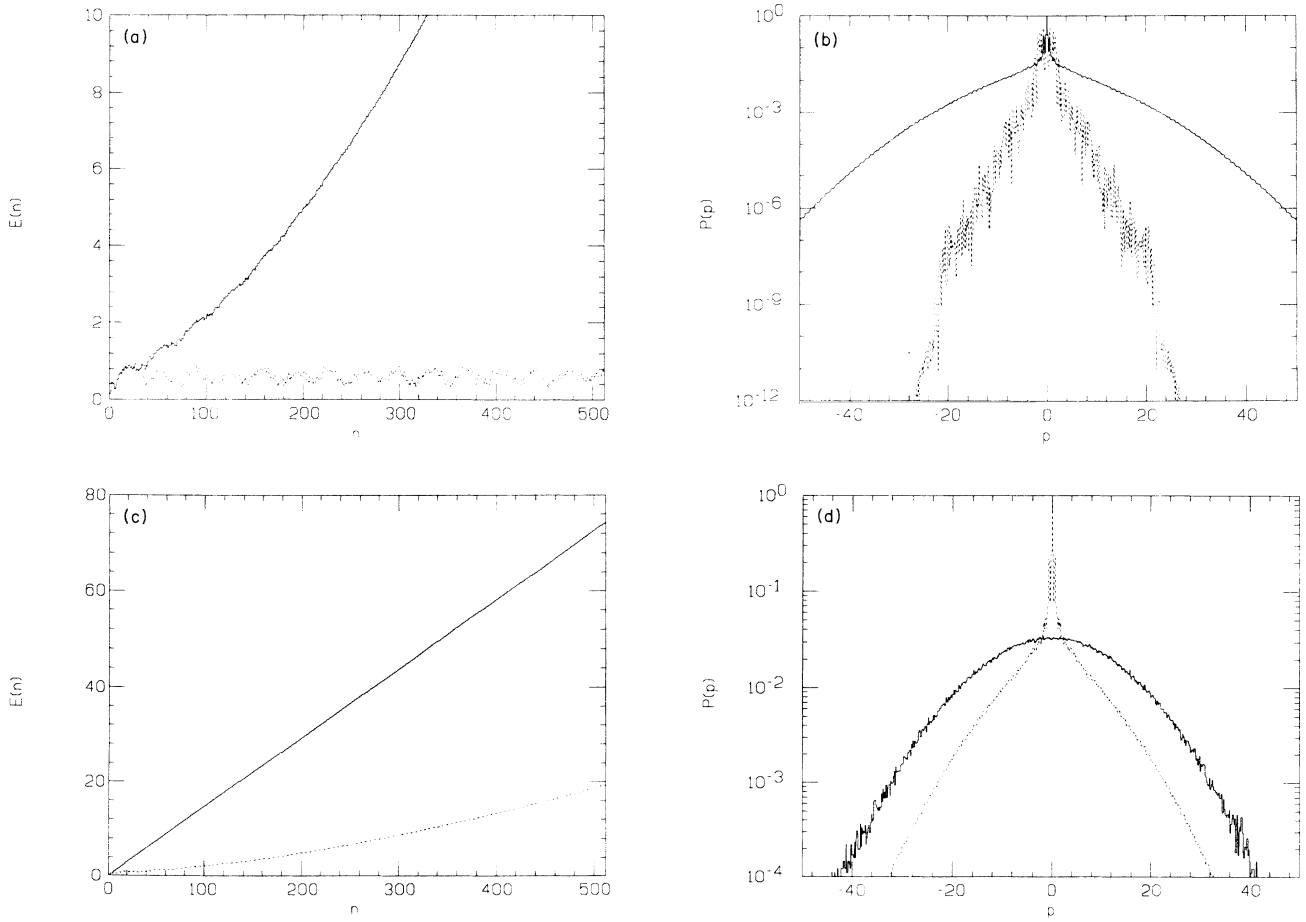

FIG. 5. Same as Fig. 1, but for the version where the mean energy is measured. The parameter values are $K=5$, $2\pi\hbar=0.1/[(\sqrt{5}-1)/2]$, and $\nu=10^{-6}$.

the nonresonant case the diffusion constant of the measured dynamics in the limit of strong coupling approaches the limiting value $D_{\rm ql}$ from *below* [cf. Eq. (4.31)], the situation is reversed here: For any finite coupling $0<\nu<1$ we find a diffusion constant higher than $D_{\rm ql}$, reaching the limit from *above* for $\nu\to 1$.

Figure 6(b) shows the corresponding distributions of action after 512 time steps. It is clearly visible how the conspicuously regular, roughly rectangular distribution function, reflecting quantum-mechanical coherence in the unmeasured resonant case, is washed out and deformed towards a Gaussian by continuous measurement.

It is, of course, tempting to combine the results for both resonant and nonresonant cases to infer how the succession of quantum resonances at rational values, and dynamical localization at irrational values of the parameter $2\pi\hbar$, is modified in the measured dynamics. While it would be prohibitively costly to investigate this in numerical detail, our results already provide good evidence for a very simple picture: In the measured dynamics, localized as well as resonant behavior is replaced, on a sufficiently long time scale, by linear diffusion. Remnants of both coherence effects, however, remain visible in *smooth* deviations of the diffusion constant, as a function of $2\pi\hbar$, from the strong coupling limit $D_{\rm ql}$: Peaks of finite width are expected at simple rational values $2\pi\hbar=p/q$, standing out against a "background" below $D_{\rm ql}$. Furthermore, it is to be expected that both the height and the width acquired by a quantum resonance under the influence of continuous measurements, will decrease rapidly as the associated rational p/q approaches an irrational number.[23]

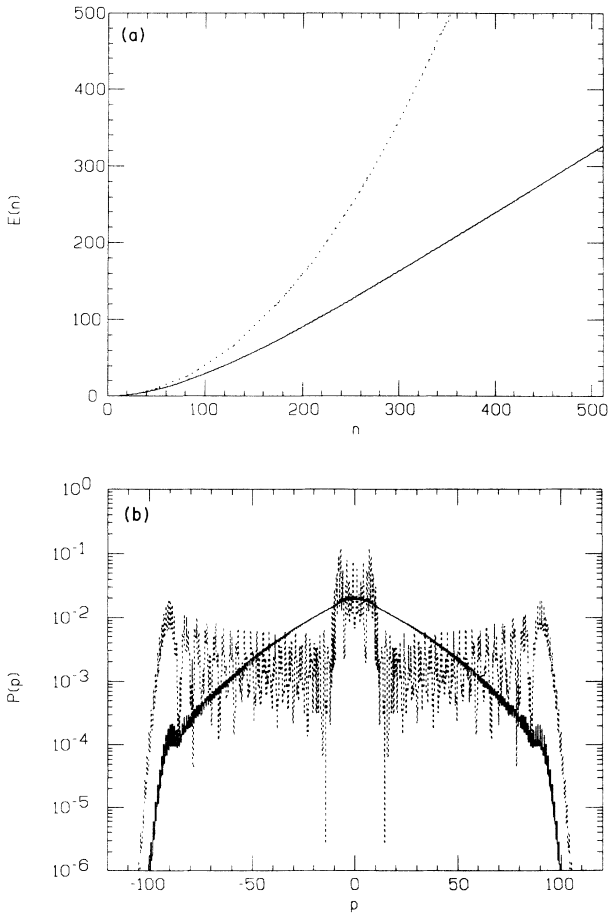

FIG. 6. Same as Fig. 1 [parts (a) and (b)] but at a quantum resonance, $2\pi\hbar=0.25$. The other parameter values are $K=5$ and $\nu=10^{-2}$.

V. CONCLUSIONS

In this paper, we have discussed models describing measurements performed on quantum systems continuously in time. We have assumed that the meter is macroscopic and couples to the measured system via a variable fluctuating rapidly on the time scale of the measured system. In this case the measured dynamics can be described by a Markovian quantum master equation which we derived in Sec. II. Its form depends on the type of quantity measured. Its parameters contain the strength of the coupling, the fluctuation strength of the coupling meter variable, and its (short) time scale. We analyzed the response of the meter to the measured system in Sec. III. Here we made the basic assumption that the response is linear, and that measurements of expectation values of suitable meter variables can be considered classical. We then analyzed the measured quantum dynamics of a classically chaotic system, the standard map, and also considered the semiclassical limit of that description. In particular we derived and solved numerically the master equations for the case when either the distribution of the action variable or its mean square are measured. In the case of strong coupling the quantum-mechanical localization effects present in the unmeasured dynamics are completely destroyed. The semiclassical description, including deterministic diffusion if the classical system is chaotic and additional strong quantum noise due to the measurement, is quantitatively satisfactory in this regime. In the case of weak coupling the semiclassical description was found to fail. Localization is preserved in the measured dynamics for sufficiently short times $n<n_c$, where n_c is characteristic of the measurement performed, but it gives way to a quantum-mechanical diffusion process for $n>n_c$. Its diffusion constant increases with the strength of the coupling, but for n_c larger than the localization time n^* (weak coupling) it remains below the constant of classical chaotic diffusion. Therefore, in contrast to the findings reported in Ref. 7, where a meter consisting of a two-level system was considered, we find that localization is always destroyed on a long time scale by the type of measurements we considered.

ACKNOWLEDGMENTS

Financial support by the Deutsche Forschungsgemeinschaft through its SFB 237 (for R.G.) and by Minerva (for T.D.) is gratefully acknowledged. One of us (T.D.) would like to thank the Department of Nuclear Physics, and in particular Professor Uzy Smilansky, for their kind

hospitality and the stimulating atmosphere enjoyed during a stay at the Weizmann Institute of Science, Rehovot, Israel.

APPENDIX

Here we wish to evaluate the kernel G_W of Eq. (4.22) in the limit $\hbar \to 0$, such that the momenta $p = 2\pi\hbar l, p' = 2\pi\hbar l'$ are held fixed. First we note that the quadruple sum of Eq. (4.22) becomes a double integral and double sum

$$\sum_{l_1', l_2', l_1, l_2} \to \frac{1}{(2\pi\hbar)^2} \int d(p_1' + p_2') \int d(p_1 + p_2) \sum_{\Delta l'} \sum_{\Delta l} \tag{A1}$$

with $\Delta l' = l_1' - l_2', \Delta l = l_1 - l_2$. Furthermore the two functions

$$\frac{\sin(\pi x/\hbar)}{(\pi x)} \to \delta(x) \tag{A2}$$

in Eq. (4.22) simplify in the limit as indicated. The two integrals over $(p_1' + p_2'), (p_1 + p_2)$ for fixed $\Delta l', \Delta l$ can therefore be carried out. The following expression then remains to be analyzed for $q, q' \in [0, 1)$:

$$G_W \left(\frac{p'}{2\pi\hbar}, q' \middle| \frac{p}{2\pi\hbar}, q \right) \simeq N \int_0^1 dx \int_0^1 dy \sum_{\Delta l'} \sum_{\Delta l} \exp 2\pi i [(\Delta l' q' - \Delta l q) - \tilde{p}\Delta l - (\tilde{p}' - \tilde{p})(x - y) - \tfrac{1}{2}(\Delta l' - \Delta l)(x + y)] \times \exp\left[\frac{iK}{4\pi^2\hbar} [\cos(2\pi x) - \cos(2\pi y)] \right] \exp[-\tfrac{1}{2} g^2 \tau_x \langle (X^{(0)})^2 \rangle [f'(\tilde{p})]^2 (\Delta l)^2] , \tag{A3}$$

where $\tilde{p} = p/2\pi\hbar$ and N is a normalization constant. We have used the explicit form of $G(l_1', l_2', | l_1, l_2)$ which follows its definition (4.21) and Eq. (4.15) and we have inserted the integral representation of b_l, Eq. (4.17). Furthermore, we expanded $[f(\tilde{p}') - f(\tilde{p})]^2 \simeq [f'(\tilde{p})]^2 (\Delta l)^2$. The sum over $\Delta l'$ yields the factor

$$\sum_{m=-\infty}^{\infty} \delta \left(q' - \frac{(x+y)}{2} - m \right) , \tag{A4}$$

i.e., $(x+y)/2$ may be replaced by q' modulo 1. The sum over Δl can also be performed and yields the factor

$$\sum_{m=-\infty}^{\infty} \frac{1}{\sqrt{2\pi\Delta(p)}} \exp\left[-\frac{(p + q - q' - m)^2}{2\Delta(p)} \right] \tag{A5}$$

with

$$\Delta(p) = g^2 \tau_x \langle (X^{(0)})^2 [f'(\tilde{p})]^2 . \tag{A6}$$

The last integral to be carried out then is over $\Delta x = x - y$,

$$\int d\,\Delta x \exp\{ -i(\Delta x/\hbar)(p' - p) - K/2\pi^2\hbar [\sin(\pi \Delta x) \sin(2\pi q')] \} \tag{A7}$$

which yields asymptotically a factor

$$\delta \left(p' - p + \frac{K}{2\pi} \sin(2\pi q') \right) . \tag{A8}$$

Collecting all factors we arrive at the result (4.23) with (4.24).

It remains to consider case (4.16) [instead of (4.15)]. Then the last factor in the integrand of Eq. (A3) is replaced by

$$[\delta_{\Delta l, 0} + \lambda(1 - \delta_{\Delta l, 0})] , \tag{A9}$$

with λ defined by Eq. (4.25), otherwise Eq. (A3) remains unchanged. The sum over Δl therefore yields a factor

$$1 - \lambda + \lambda \sum_{m=-\infty}^{\infty} \delta(p + q - q' - m) \tag{A10}$$

in agreement with Eq. (4.28).

*Present address: Institut für Physik, Universität Augsburg, Memminger Strasse 6, D-8900 Augsburg, West Germany.

[1] John von Neumann, *Die Mathematischen Grundlagen der Quantenmechanik* (Springer, Berlin, 1934).
[2] *Quantum Theory and Measurement*, edited by J. A. Wheeler and W. H. Zurek (Princeton University Press, Princeton, 1983).
[3] W. E. Lamb, Jr., in *Quantum Measurement and Chaos*, edited by E. R. Pike and S. Sarkar (Plenum, New York, 1987).
[4] C. M. Caves, Phys. Rev. D **33**, 1643 (1986); **35**, 1815 (1986).
[5] A. Schmid, Ann. Phys. (N.Y.) **173**, 103 (1987).
[6] C. M. Caves and G. J. Milburn, Phys. Rev. A **36**, 5543 (1987).
[7] S. Sarkar and S. Satchell, Europhys. Lett. **1**, 133 (1987); J. Phys. A **20**, L437 (1987); Physica **29D**, 343 (1988).
[8] B. C. Sanders and C. J. Milburn (unpublished).
[9] *Quantum Optics, Experimental Gravitation, and Measurement Theory*, edited by P. Meystre and M. O. Scully (Plenum, New York , 1983).
[10] W. E. Lamb, Jr., in *Chaotic Behaviour in Quantum Systems*, edited by G. Casati (Plenum, New York, 1985).
[11] G. Casati, B. V. Chirikov, F. M. Izrailev, and J. Ford, in *Lecture Notes in Physics* (Springer, Berlin, 1979); vol. 93, p. 334; S. Fishman, D. R. Grempel, and R. E. Prange, Phys. Rev. Lett. **49**, 509; Phys. Rev. A **29**, 1639 (1984).

[12]J. D. Hanson, E. Ott, and M. Antonsen, Jr., Phys. Rev. A **29**, 1819 (1984); S. Adachi, M. Toda, and K. Ikeda, Phys. Rev. Lett. **61**, 659 (1988).

[13]T. Dittrich and R. Graham, Z. Phys. B **62**, 515 (1986); Europhys. Lett. **4**, 263 (1987); **7**, 287 (1988).

[14]T. Dittrich and R. Graham, in *Instabilities and Nonequilibrium Structures II*, edited by E. Tirapegui and D. Villaroel (Kluwer Academy, Dordrecht, 1989).

[15]T. Dittrich and R. Graham, Ann. Phys. (N.Y.) **200**, 363 (1990).

[16]B. V. Chirikov, Phys. Rep. **52**, 263 (1979).

[17]B. V. Chirikov, in *Chaos and Quantum Physics*, Proceedings of Session LII of the Les Houches Summer School, edited by A. Voros and M.-J. Giannoni (North-Holland, Amsterdam, 1990).

[18]M. V. Berry, Trans. R. Soc. (London) Ser. A **287**, 237 (1977).

[19]C. Froeschlé, Astrophys. Space Sci. **37**, 87 (1975); B. V. Chirikov, Fiz. Plazmy **5**, 880 (1979) [Sov. J. Plasma Phys. **5**, 492 (1979)].

[20]C. F. F. Karney, A. B. Rechester, and R. B. White, Physica **4D**, 425 (1982).

[21]A. J. Lichtenberg and M. A. Lieberman, *Regular and Stochastic Motion* (Springer, Berlin, 1983).

[22]F. M. Izrailev and D. L. Shepelyansky, Dokl. Akad. Nauk. SSSR **249**, 1103 (1979) [Sov. Phys.—Dokl. **24**, 996 (1979)]; Teor. Mat. Fiz. **43**, 417 (1980) [Theor. Math. Phys. **43**, 553 (1980)].

[23]G. Casati, J. Ford, I. Guarneri, and J. Vivaldi, Phys. Rev. A **34**, 1413 (1986).